Title
Attribution of the July–August 2013 heat event in Central and Eastern China to anthropogenic greenhouse gas emissions

Journal
Environmental Research Letters, 12(5)

ISSN
1748-9318

Authors
Ma, Shuangmei
Zhou, Tianjun
Stone, Dáithí A
et al.

Publication Date
2017-05-01

DOI
10.1088/1748-9326/aa69d2

Peer reviewed

Attribution of the July–August 2013 heat event in Central and Eastern China to anthropogenic greenhouse gas emissions

2017 Environ. Res. Lett. 12 054020

(http://iopscience.iop.org/1748-9326/12/5/054020)

Environmental Research Letters

OPEN ACCESS

RECEIVED
18 July 2016

REVISED
27 March 2017

ACCEPTED FOR PUBLICATION
29 March 2017

PUBLISHED
19 May 2017

LETTER

Attribution of the July–August 2013 heat event in Central and Eastern China to anthropogenic greenhouse gas emissions

Shuangmei Ma[1,2,3], **Tianjun Zhou**[2,3,4], **Dáithí A Stone**[5], **Oliver Angélil**[6] **and Hideo Shiogama**[7]

1 Institute of Climate System, Chinese Academy of Meteorological Sciences, Beijing 100081, People's Republic of China
2 LASG, Institute of Atmospheric Physics, Chinese Academy of Sciences, Beijing 100029, People's Republic of China
3 University of Chinese Academy of Sciences, Beijing 100049, People's Republic of China
4 Jiangsu Collaborative Innovation Center for Climate Change, Nanjing, People's Republic of China
5 Lawrence Berkeley National Laboratory, Berkeley, CA 94720, United States of America
6 Climate Change Research Centre and ARC Centre of Excellence for Climate System Science, UNSW Australia, Sydney NSW 2052, Australia
7 National Institute for Environmental Studies, Ibaraki 305-8506, Japan

E-mail: zhoutj@lasg.iap.ac.cn

Keywords: attribution, internal variability, human influence

Supplementary material for this article is available online

Abstract

In the midsummer of 2013, Central and Eastern China (CEC) was hit by an extraordinary heat event, with the region experiencing the warmest July–August on record. To explore how human-induced greenhouse gas emissions and natural internal variability contributed to this heat event, we compare observed July–August mean surface air temperature with that simulated by climate models. We find that both atmospheric natural variability and anthropogenic factors contributed to this heat event. This extreme warm midsummer was associated with a positive high-pressure anomaly that was closely related to the stochastic behavior of atmospheric circulation. Diagnosis of CMIP5 models and large ensembles of two atmospheric models indicates that human influence has substantially increased the chance of warm mid-summers such as 2013 in CEC, although the exact estimated increase depends on the selection of climate models.

1. Introduction

Extreme weather or climate events, such as droughts, floods, heavy precipitation, heat waves, cold spells, and tropical and extratropical storms, have always been an inherent part of the climate and been a matter of concern to decision and policy makers because such events are likely to destabilize ecosystems and affect human lives and activities, such as food production, transportation infrastructure, and water management.

Global warming is unequivocal (IPCC 2013). A changing climate leads to changes in the frequency, intensity, spatial extent, duration, and timing of extreme weather and climate events, and it can result in unprecedented extreme weather and climate events (IPCC 2012). More frequent and severe extreme weather and climate events, such as extreme heat, and intense precipitation and drought, have been observed since about 1950 (Perkins *et al* 2012, IPCC 2013, Fischer and Knutti 2014) and are evident in climate model projections (Fischer *et al* 2013, Sillmann *et al* 2013). The higher frequency of extreme weather or climate events such as deadly heat waves and devastating floods and droughts has sparked interest in understanding the role of the anthropogenic contribution. The human influence on the increasing (decreasing) severity of extremely warm (cold) nights and days and the intensification of precipitation extremes is detectable on a global scale (Christidis *et al* 2011, Min *et al* 2011, 2013, Wen *et al* 2013, Zhang *et al* 2013, Fischer and Knutti 2014, Christidis and Stott 2016). Analyses based on a probabilistic attribution framework suggest that human-induced climate change has generally increased the probability of heat waves as well as drought and heavy precipitation events (Stott *et al* 2004, Pall *et al* 2011, Rahmstorf and Coumou 2011, Lewis and Karoly 2013, 2015, Imada *et al* 2014, Lestari *et al* 2014, Wolski *et al* 2014, Fischer and Knutti 2015, King *et al* 2015).

Although the probability of extreme events which can be attributable to anthropogenic greenhouse gas emissions is sensitive to the spatial and temporal scale of the event, attribution statements can serve as a proxy for similar events occurring at different temporal and spatial scales (Angélil *et al* 2014). An extreme weather or climate event can occur because of internal natural variability; thus, it is impossible to firmly attribute an extreme event to solely human influence. The same extreme event can be considered 'mostly natural' when viewed in terms of anomalous magnitude and 'mostly anthropogenic' when viewed in terms of occurrence probability (Imada *et al* 2013, 2014, Otto *et al* 2012). Similarly, while anthropogenic influence may be almost necessary for an extremely hot event to occur nowadays, it is hardly sufficient for the occurrence at present, with natural variability rather being the dominant determinant (Hannart *et al* 2016). Despite the large irreducible uncertainties at local to regional scale as a result of natural internal variability, the chances of high-temperature extremes are expected to dramatically increase globally (Christidis *et al* 2015, Fischer *et al* 2013, Fischer and Knutti 2015). Meanwhile, due to the limited realizations of rare events in observations and structural deficiencies of models, each individual event attribution is subject to uncertainty, but the reliability of event attribution can be improved by using complementary methods to estimate the probability of extreme events (Hegerl 2015).

Central and Eastern China (CEC) was affected by a severe heat event during July and August of 2013. This was the strongest heat event since at least 1951 and it resulted in serious summer drought and crop growth was affected, the water and electricity supply were interrupted, and people were hospitalized for heat-related symptoms (CMA 2014). It is estimated that anthropogenic influence has increased the likelihood of extreme hot summers in Eastern China, and it is projected that similarly hot summers will become more frequent in the future (Sun *et al* 2014). However, despite the discernible impact of anthropogenic forcing, the contribution of internal variability to the hot midsummer of 2013 over CEC is also important (Zhou *et al* 2014). Therefore, in this study, we aim to assess the relative contributions of human influence and internal natural variability to the high surface air temperature (SAT) anomalies during July–August of 2013 over CEC. To achieve this goal and improve the reliability of attribution results, both the Coupled Model Intercomparison Project phase 5 (CMIP5) model results and the International CLIVAR C20C+ Detection and Attribution simulations are used. We find that while this heat event is an event dominated by natural variability, the anthropogenic influence has significantly increased the chance of such kinds of events, ranging from two-fold estimated by CMIP5 models, to seventeen-fold and four-fold estimated by the CAM5.1 and MIROC5 C20C+ models, respectively.

2. Data and method

2.1. Data description

Daily maximum SATs and monthly mean SATs at 756 stations from China's National Meteorological Information Center (NMIC, http://cdc.nmic.cn/home.do) are used. Although the data cover the period of 1951–2014, data prior to 1955 are not used because the first national standard for meteorological observations was put in place in 1955 and many stations had no records before 1955. Before the area-weighted mean temperature is calculated, the station data are interpolated onto a $0.5° \times 0.5°$ resolution grid using iterative improvement objective analysis with a search radius of 3°–2°–1°–0.5° using the 'obj_anal_ic_Wrap' function in the NCAR Command Language (NCL) (NCAR 2012). Monthly 500 hPa geopotential height (Z500) data obtained from the ERA-Interim reanalysis (Dee *et al* 2011) are also used.

To allow for the different model representations of the climate system, we use monthly data generated by the atmospheric general circulation models (AGCMs) CAM5.1 (Angélil *et al* 2017) and MIROC5 (Shiogama *et al* 2013, 2014), run at a resolution of 1° and 1.4°, respectively, provided by the International CLIVAR Climate of the 20th Century Plus Detection and Attribution Project (C20C + D&A). Two scenarios are examined (table S1 available at stacks.iop.org/ERL/12/054020/mmedia): All-Hist and Nat-Hist. In the All-Hist scenario, CAM5.1 and MIROC5 are forced by historical anthropogenic and natural external forcing agents plus observational data of sea surface temperature (SST) and sea ice (All-Hist). In the Nat-Hist scenario, the anthropogenic radiative forcings (and land cover/use for MIROC5) are set to mid-19th century values and the observed SSTs and sea ice are adjusted according to an estimate of the seasonally-varying of the warming attributable to anthropogenic forcing (Nat-Hist) (Stone and Pall 2016). For CAM5.1, both All-Hist and Nat-Hist include 400 realizations, including a 50-member ensemble from January 1959 to Jun 2015, a 50-member ensemble from January 1996 to Jun 2015, and a 300-member ensemble from January 2010 to Jun 2015. For MIROC5, All-Hist includes a 10-member ensemble from January 1950 to December 2014, a 50-member ensemble from January 2006 to Oct 2015, and a 50-member ensemble from Jan 2010 to Oct 2015; Nat-Hist includes a 50-member ensemble from January 2006 to Aug 2015 and a 50-member ensemble from 2010 Jan to Aug 2015. Each realization in the scenarios differs from the other only in its initial state. For more details about the experimental design, the reader is referred to http://portal.nersc.gov/c20c/. Outputs of these simulations are available from this website.

To investigate the dependence of the attribution results on the experiment design, the monthly SATs simulated by the historical, historicalNat, RCP8.5, and piControl experiments from the fifth phase of the

Coupled Model Intercomparison Project (CMIP5) (Taylor *et al* 2012) are analyzed. The historical simulations are forced by natural (solar radiation and volcanic aerosols) and anthropogenic agents (greenhouse gases, aerosols, ozone, and land use), while the historicalNat simulations are only forced by natural agents. The RCP8.5 simulations are run with projected increases in greenhouse gases and represent the high emission scenario that is the most representative of global CO_2 emissions from 2005 to present, whereas the piControl simulations are forced with the external forcing fixed at 1850 levels. We select 17 CMIP5 models for which historical, historicalNat, RCP8.5, and piControl simulations are available (table S2). To examine the anthropogenic influence on odds of the 2013 midsummer extreme high-temperature event over CEC, both the historicalNat and piControl simulations are used as an indicator of variability without any anthropogenic impact.

2.2. Method

The probability ratio (PR) and fraction of attributable risk (FAR) are defined as follows (Stone and Allen 2005, Fischer and Knutti 2015):

$$\mathrm{PR} = P_{\mathrm{All}}/P_{\mathrm{Nat}} \tag{1}$$

$$\mathrm{FAR} = 1 - (P_{\mathrm{Nat}}/P_{\mathrm{All}}) \tag{2}$$

where P_{Nat} is the probability of an event occurring in the counterfactual natural scenario (estimated from simulations without anthropogenic influence) and P_{All} is the corresponding probability under the factual scenario (calculated using simulations with anthropogenic influence included). PR is the factor by which the probability of an event has changed under anthropogenic forcing, and FAR is the fractional contribution of human activity to a particular event. The uncertainties of PR and FAR are estimated using the 'basic bootstrap confidence interval' method and corresponding best estimates are approximated by the median.

3. Results

3.1. Observed characteristics of the 2013 summer heat event in CEC

CEC was hit by a heat event in July–August of 2013. The number of heat-wave days (daily maximum temperature ≥ 35 °C) in 2013 was greater than 30 d over large areas of CEC and even exceeded 50 d over the lower reaches of the Yangtze River (figure 1(*a*)). During the 2013 midsummer, most CEC regions experienced more 10 heat-wave days than the 1961–1990 long-term average (figure 1(*b*)). The regionally averaged number of the heat-wave days over CEC in 2013 was the highest since observations were standardized in 1955 (figure 1(*c*)). For many CEC stations, daily maximum temperatures in July–August of 2013 reached or exceeded the standard of the extreme temperature threshold (defined as the 95th percentile of the daily maximum temperatures for 1961–1990) and even broke the record (figure 1(*d*)). The July–August 2013 mean SAT was warmer than normal by as much as 3 °C over parts of CEC and the 2013 midsummer was the hottest on record. The regionally averaged SAT reached 28.14 °C (figures 1(*e*) and (*f*)) and exceeded the observed 1961–1990 climatology by 1.89 °C (figure 2(*f*)).

As shown in figure 2(*a*), in terms of the anomalies of the 2013 July–August mean SAT and the geopotential height at 500 hPa (Z500), the hot midsummer of 2013 in CEC was associated with positive anomalies of Z500, which induced descending motion and reduced cloudiness and favored the formation of warm air at the surface.

To avoid the dependence of attribution results on the observational products, we also examine the observed characteristics of the 2013 July–August heat event in CEC derived from National Aeronautics and Space Administration (NASA) Goddard Institute for Space Studies Surface Temperature Analysis (GISTEMP) (Hansen *et al* 2010) and UK Hadley Centre's HadCRUT4 (Morice *et al* 2012), and compare with those derived from NMIC station observation. The observed characteristics of the 2013 mid-summer extremely high temperature revealed by GISTEMP and HadCRUT4 are highly consistent with those described by station data from China's NMIC (figure not shown). Thus, in this study, only the NMIC station temperature data set is further used for attribution analyses.

3.2. July–August of 2013 temperature simulations with CAM5.1 and MIROC5

In terms of the time evolution of the regionally averaged July–August SAT anomalies in CEC during 1959–2014, both AGCMs reproduce the annual variability to some extent (figures 2(*f*) and S1(*f*)). The model ensemble mean of SAT anomalies in CEC positively correlate with the observations with correlation coefficient of 0.51 (0.52 after linear detrending) for CAM5.1 and 0.53 (0.51 after linear detrending) for MIROC5, respectively, and are statistically significant from zero at the 0.01 level. In addition, both AGCMs reproduce the observed warming since the 1980s.

In terms of the July–August SAT anomaly pattern, the ensemble average of all All-Hist members for 2013 in CAM5.1 and MIROC5 does not capture the extremely high July–August mean SAT anomaly in CEC (shading in figures 2(*b*) and S1(*b*)). Moreover, the observed positive high-pressure anomaly center at Z500 in the northeast of CEC lies eastward to the Western Pacific in CAM5.1 and westward to the Northwestern China in MIROC5 in the All-Hist ensemble mean of all 2013 members (contours in figures 2(*b*) and S1(*b*)). However, for the average of

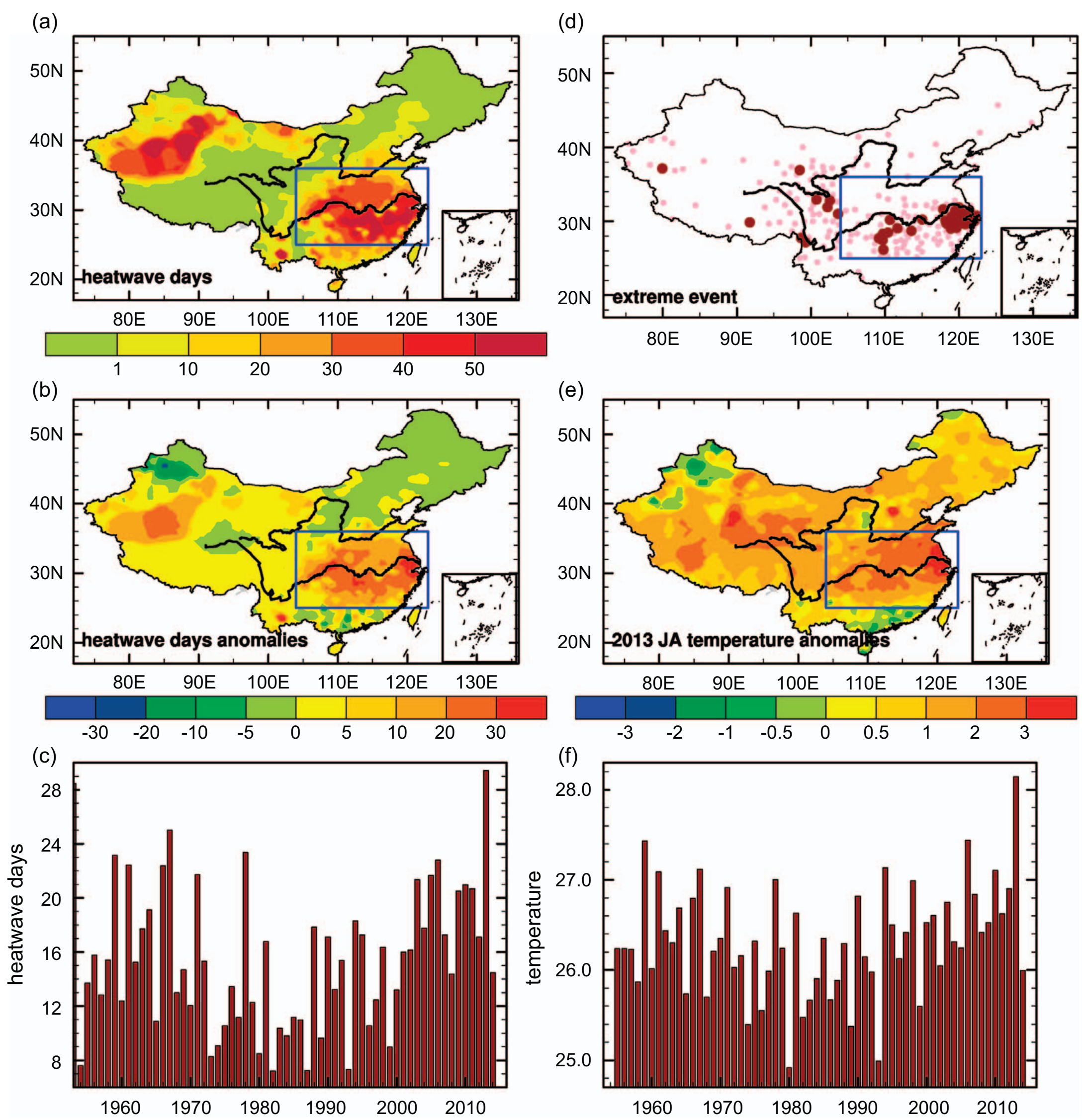

Figure 1. Observed characteristics of the 2013 summer heat event. (*a*) Number of heat-wave days (daily maximum temperature T_{max} ≥ 35 °C) in 2013. (*b*) The 2013 anomalous number of heat-wave days (relative to the mean for 1961–1990). (*c*) July–August mean heat-wave days during 1955–2014 averaged over Central and Eastern China, shown as the rectangular box in (*a*)–(*b*) bounded by 104°–123°E and 25°–36°N. (*d*) Stations (firebrick color) for which 2013 midsummer (July–August) daily maximum temperatures exceeded the observed records and stations (light pink color) with midsummer daily maximum temperatures that reached or exceeded the threshold of extreme temperature, which is defined as the 95th percentile of the daily maximum temperatures for 1961–1990 during July–August. (*e*) 2013 July–August mean surface air temperature anomalies (°C) relative to the mean for 1961–1990. (*f*) Time series of the July–August mean surface air temperature averaged over Central and Eastern China.

the members with the largest positively July–August SAT anomalies in CEC in 2013, the July–August SAT and Z500 anomalies show similar patterns with observations (figures 2(*c*) and S1(*c*)). Furthermore, the All-Hist ensemble spread of the July–August mean SAT and Z500 anomalies in 2013 are the largest in the CEC in CAM5.1 and MIROC5. The first leading empirical orthogonal function (EOF), accounting for 35% (28%) of the total variance of the intra-ensemble SAT (Z500) anomalies in CAM5.1 and 34% (30%) of the total variance of the intra-ensemble SAT (Z500) anomalies in MIROC5, has a maximum center in CEC (figures 2(*d*) and (*e*), S1(*d*), S1(*e*)). This indicates that the observed 2013 July–August high-temperature and high-pressure anomalies in CEC were not deterministically forced by the boundary conditions that included the observed changes in greenhouse gas concentrations, anthropogenic and natural aerosols, ozone, solar luminosity, land cover, SST, and sea ice. Instead, the stochastic behavior of atmospheric circulation was related to the observed extremely warm July–August SAT and positive high-pressure anomalies over CEC in 2013.

3.3. Anthropogenic influence on the occurrence probability of the observed 2013 heat event

Although the particular climate extreme event cannot be categorically ascribed to the effect of human activity on climate, the role of anthropogenic influence to the change in the odds of the occurrence of a climate extreme event is identifiable.

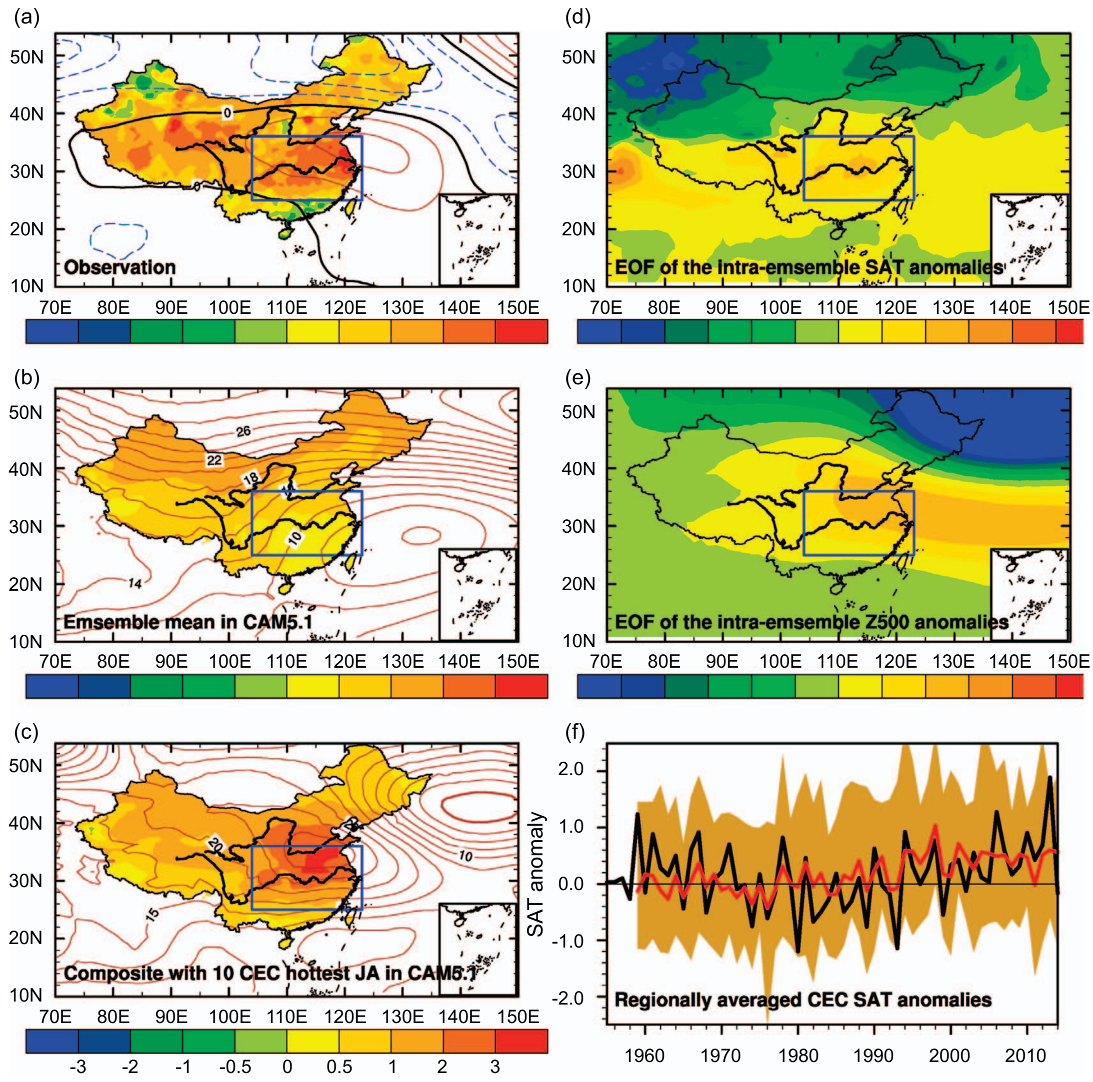

Figure 2. 2013 July–August mean surface air temperature (SAT) anomalies (°C, shaded) and geopotential height anomalies at 500 hPa (Z500, units in m, contours) relative to the base period for (*a*) observations, the ensemble mean of (*b*) all CAM5.1 ALL-Hist members and (*c*) only the 10 ALL-Hist members with the warmest 2013 midsummers in Central and Eastern China. (*d*) The first EOF of the intra-ensemble of CAM5.1 ALL-Hist for 2013 July–August SAT anomalies. (*e*) Same as (*d*) but for Z500. (*f*) Time series of July–August SAT anomalies during 1955–2014 averaged over Central and Eastern China denoted by the blue rectangle box in (*a*)–(*e*) for the observations (black line) and CAM5.1 ALL-Hist 50-member ensemble mean (red line), with the ensemble spreads (goldenrod color). Except the Z500 anomalies in (*a*) derived from the ERA-Interim reanalysis relative to the 1979–2008 base period, all other anomalies are relative to the 1961–1990 base period.

First, we show the histogram and empirical probability density functions (PDFs) of the July–August mean SAT anomalies in CEC for 1959–2014 in the observations and the All-Hist simulations of AGCMs (denoted as ALL-long). The PDFs were estimated using a kernel smoothing function. Both CAM5.1 and MIROC5 accurately simulate the distribution of the July–August mean SAT anomalies in CEC during 1959–2014 (figure 3). The observed and simulated PDFs of the July–August mean SAT anomalies in CEC during 1959–2013 are statistically indistinguishable at the 0.05 level based on a two-sided Kolmogorov-Smirnov (KS) test. The good performance of CAM5.1 and MIROC5 provides the basis to evaluate the anthropogenic contribution to the likelihood of the 2013 heat event in CEC.

The histograms and PDFs of the 2013 July–August SAT anomalies of the 400-member realizations of the CAM5.1 All-Hist and Nat-Hist, and the 110-member (100-member) realizations of the MIROC5 All-Hist (Nat-Hist) are shown in figure 3. For both All-Hist and Nat-Hist ensembles, the range of the distribution of the 2013 July–August SAT anomalies spans negative to positive values and includes the observed 2013 midsummer warm anomaly. This highlights the importance of internally generated atmospheric variability for the occurrence of the 2013 July–August heat event. There is an obvious rightward shift of the histograms and PDFs of the 2013 July–August SAT anomalies in All-Hist compared with Nat-Hist, suggesting that human influence has increased the probability of midsummer warm events. Relative to the 2013 Nat-Hist, the best-estimate PR and FAR are 17.83 and 0.94 (5th–95th percentile of 10.68–20.05 and 0.89–0.97) for CAM5.1 and 4.45 and 0.78 (5th–95th percentile of 1.61–9.86 and 0.38–0.97)

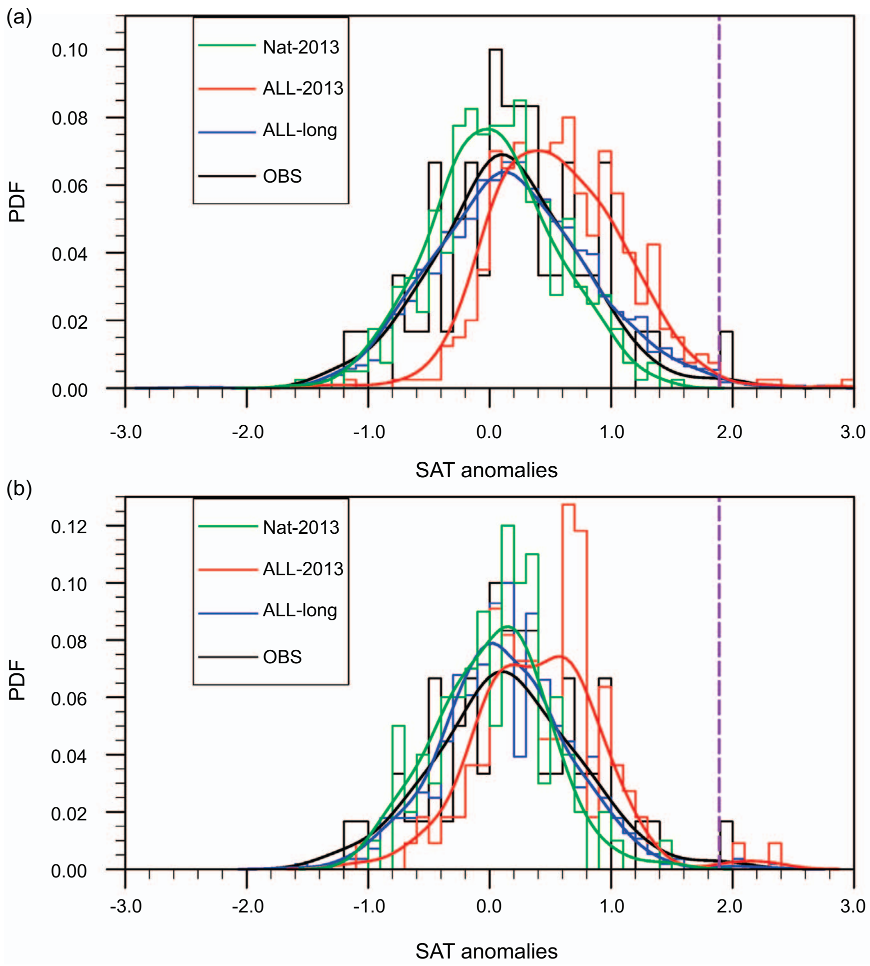

Figure 3. Histogram (bars) and probability density functions (PDFs, curve) of July–August mean SAT anomalies averaged over Central and Eastern China during 1959–2013 for observations (black bars and curve, denoted as 'OBS') and ensemble mean of (*a*) the 50-member realization in CAM5.1 ALL-Hist and (*b*) the 10-member realization in MIROC5 ALL-Hist (blue bars and curve, denoted as 'ALL-long'). Red bars (curves) are the histograms (PDF) of 2013 July–August mean SAT anomalies for the 400-members of CAM5.1 ALL-Hist in (*a*) and 60-members of MIROC5 ALL-Hist in (*b*), as indicated by 'ALL-2013.' Green bars (curves) are the histograms (PDF) of 2013 July–August mean SAT anomalies for the 400-members of CAM5.1 Nat-Hist in (*a*) and 50-members of MIROC5 Nat-Hist in (*b*), as indicated by 'Nat-2013.' The PDFs are nonparametric curves using kernel density estimation and a Gaussian smoother. The vertical purple line in (*a*) and (*b*) is the observed 2013 July–August SAT anomaly.

for MIROC5, respectively. CAM5.1 (4.1 °C, Meehl *et al* 2013) has a higher climate sensitivity than MIROC5 (2.7 °C). This difference of climate sensitivity may explain greater land warming in CAM5.1 than MIROC5. Additionally, CAM5.1 uses prescribed aerosol fields while MIROC simulates aerosol distributions based on emissions. Therefore, current weather in MIROC5 can influence aerosols while in CAM5.1 it cannot. This can influence feedbacks which are important in the simulation of extremes. Thus, stronger aerosol cooling in MIROC5 than CAM5.1 may also contribute to the lower PR and FAR for MIROC5.

Clearly, there is more than fourfold increase in the chance of extremely high temperature events, such as the 2013 July–August heat event in CEC, owing to anthropogenic influence. Although the estimated PR and FAR are sensitive to the AGCMs, the difference in the distribution of the 2013 July–August mean SATs between All-Hist and Nat-Hist in both AGCMs suggests that human activity has contributed to the probability of the extremely warm midsummers such as the 2013 July–August high temperature in CEC.

The atmospheric responses in CAM5.1 and MIROC5 may be subject to the uncertainty in the estimated anthropogenic warming patterns of sea surface temperature (Imada *et al* 2014). Thus, to increase the confidence in the attribution statements based on CAM5.1 and MIROC5, the change in the probability of the extremely high temperature event (such as the 2013 midsummer heat event in CEC) was additionally calculated with the CMIP5 simulations. The observed July–August mean SAT anomalies in CEC are well within the CMIP5 ensemble spread (figure 4(*a*)). The observed warming trend since the 1980s agrees well with the multi−model mean (MME) trend in the CMIP5 historical and RCP8.5 simulations.

In addition, as shown in figure 4(*b*), there is strong agreement in the PDF of the July–August mean SAT

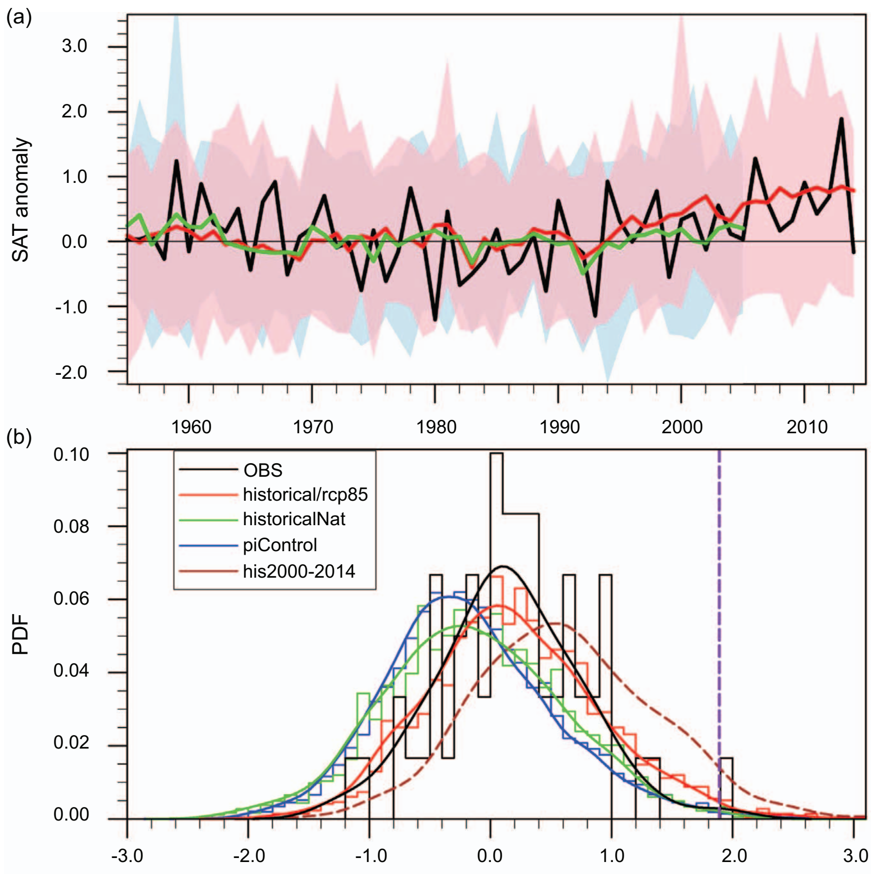

Figure 4. (*a*) Time series of observed and simulated July–August SAT anomalies averaged over Central and Eastern China during 1955–2014. Black line is for the observations, red (green) line is for the 17 CMIP5 climate models ensemble mean of historical and RCP8.5 (historicalNat) simulations. Light pink and light blue shading denote the 5th–95th percentiles of SAT among the 17 CMIP5 models. (*b*) Histogram and probability density functions (PDFs) of July–August mean SAT anomalies (relative to 1961–1990) for the observations (black bars and curve) and CMIP5 simulations of historical and RCP8.5 (red bars and curve, denoted as 'historical/rcp85') during 1955–2014, historicalNat simulations (green bars and curve) for 1955–2005, and piControl simulations (blue bars and curve, relative to the long-term mean). Dashed brown line in (*b*) indicates the simulated PDF of historical and RCP8.5 simulations for 2000–2014.

anomalies in CEC between the MME of the CMIP5 historical data and RCP8.5 simulations and observations. Based on the two-sided Kolmogorov test, the observed and simulated PDFs during 1955–2014 are not significant different at the 0.05 level. On the other hand, there are no cases of the observed value lying outside the spread of the simulations in figure 4(*a*) when approximately six cases would normally be expected. These seemingly contradictory assessments arise because the observed time series shows a considerable decadal time scale variability with respect to the CMIP5 mean time series. This may imply that the models are producing too much high frequency variability at the expense of low frequency variability, but it could also be that the large degree of lag correlation weakens the power of both tests.

There is a clear warm shift in figure 4(*b*) in the PDF of the July–August SAT anomalies in the historical data and RCP8.5 simulations and observations during 1955–2014, compared with the SAT distribution in the historicalNat and piControl simulations. The PDF of historical and RCP8.5 runs after 2000 (for 2000–2014) show a more rightward shift than that during 1955–2014.

Using the historicalNat and piControl simulations to complement the anthropogenically forced simulations, PR and FAR estimates were made. For an inherently conservative analysis, the PR and FAR were estimated using simulations of historical and RCP8.5 during 1955–2014. The best-estimated PR and FAR that correspond to the historicalNat (piControl) simulations are 2.38 and 0.58 (2.29 and 0.56), with 5th−95th percentage range of 1.88–3.1 and 0.47–0.68 (1.98–2.68 and 0.49–0.63), respectively. This means that human influence has increased the probability of extreme high-temperature events, such as the 2013 July–August heat event in CEC, by about two times, and that 60% of this heat event is attributable to anthropogenic influence.

4. Summary

CEC experienced the warmest midsummer on record in 2013. In this study, we used the CAM5.1 and MIROC5 models provided by the International CLIVAR C20C+ Detection and Attribution Project and simulations with CMIP5 models to analyze how anthropogenic emissions and natural internal atmospheric variability contributed to the midsummer heat event in 2013 in CEC. The results suggest that the internal atmospheric variability and human activities strongly contributed to the 2013 midsummer heat event in CEC.

The 2013 July–August warm midsummer was associated with a positive high-pressure anomaly that was closely related to the stochastic behavior of atmospheric circulation. This result is robust and verified by both AGCM models.

The anthropogenic influence on climate has increased the probability of midsummer events with extreme heat, such as the 2013 July–August high-temperature event in CEC, by a factor of seventeen (four), based on the detection and attribution simulations of CAM5.1 (MIROC5), and it has about doubled the chance of such extreme heat events according to analysis of the CMIP5 simulations.

Probabilistic attribution of warm midsummer in CEC, as in 2013, with CAM5.1, MIROC5 and output from the CMIP5 models, all suggest a positive attribution statement, i.e. increased odds of the event as a consequence of anthropogenic activity.

Acknowledgments

T Zhou and S Ma are supported by National Natural Science Foundation of China under Grant Nos. 41330423, 41420104006, and R&D Special Fund for Public Welfare Industry (meteorology) under Grant Nos. GYHY201506012, and GYHY201406020. H Shiogama was supported by the Program for Risk Information on Climate Change from the Ministry of Education, Culture, Sports, Science and Technology of Japan. The Earth Simulator at JAMSTEC and NEC SX at NIES were used to perform the MIROC5 simulations.

References

Angélil O *et al* 2014 Attribution of extreme weather to anthropogenic greenhouse gas emissions: sensitivity to spatial and temporal scales *Geophys. Res. Lett.* **41** 2150–5

Angelil O *et al* 2017 An independent assessment of anthropogenic attribution statements for recent extreme weather *J. Clim.* **30** 5–16

Christidis N *et al* 2015 Dramatically increasing chance of extremely hot summers since the 2003 European heatwave *Nat. Clim. Change* **5** 46–50

Christidis N, Stott P A and Brown S J 2011 The role of human activity in the recent warming of extremely warm daytime temperatures *J. Clim.* **24** 1922–30

Christidis N and Stott P A 2016 Attribution analyses of temperature extremes using a set of 16 indices *Weather Clim. Extremes* **14** 24–35

CMA 2014 China Climate Bulletin for 2013 *China Meteorological Administration* 50 pp

Dee D P *et al* 2011 The ERA-Interim reanalysis: configuration and performance of the data assimilation system *J. Roy. Meteor. Soc.* **137** 553–97

Fischer E M and Knutti R 2015 Anthropogenic contribution to global occurrence of heavy-precipitation and high-temperature extremes *Nat. Clim. Change* **5** 560–4

Fischer E M and Knutti R 2014 Detection of spatially aggregated changes in temperature and precipitation extremes *Geophys. Res. Lett.* **41** 547–54

Fischer E, Beyerle U and Knutti R 2013 Robust spatially aggregated projections of climate extremes *Nat. Clim. Change* **3** 1033–38

Hannart A, Pearl J, Otto F E L, Naveau P and Ghil M 2016 Causal counterfactual theory for the attribution of weather and climate-related events *Bull. Am. Meteorol. Soc.* **97** 99–110

Hansen J *et al* 2010 Global surface temperature change *Rev. Geophys.* **48** RG4004

Hegerl G C 2015 Use of models and observations in event attribution *Environ. Res. Lett.* **10** 071001

Imada Y, Shiogama H, Watanabe M, Mori M, Kamae Y, Ishii M and Kimoto M 2014 The contribution of anthropogenic forcing to the Japanese heat waves of 2013. explaining extreme events of 2013 from a climate perspective *Bull. Am. Meteorol. Soc.* **95** S52–4

Imada Y, Watanabe M, Mori M, Kimoto M, Shiogama H and Ishii M 2013 Contribution of atmospheric circulation change to the 2012 heavy rainfall in southern Japan. *Bull. Am. Meteorol. Soc.* **94** S52–4

IPCC 2012 Summary for policymakers. *A Special Report of Working Groups I and II of the Intergovernmental Panel on Climate Change* ed C B Field *et al* (Cambridge: Cambridge University Press) pp 3–21

IPCC 2013 Summary for policymakers *Climate Change 2013: The Physical Science Basis Contribution of Working Group I to the Fifth Assessment Report of the Intergovernmental Panel on Climate Change* ed T F Stocker, D Qin, G-K Plattner, M Tignor, S K Allen, J Boschung, A Nauels, Y Xia, V Bex and P M Midgley (Cambridge: Cambridge University Press)

King A D *et al* 2015 Attribution of the record high central England temperature of 2014 to anthropogenic influences *Environ. Res. Lett.* **10** 054002

Lestari R K and Kimoto M *et al* 2014 Increasing potential of biomass burning over Sumatra, Indonesia induced by anthropogenic tropical warming *Environ. Res. Lett.* **9** 104010

Lewis S C and Karoly D J 2013 Anthropogenic contributions to Australia's record summer temperatures of 2013 *Geophys. Res. Lett* **40** 3705–9

Lewis S C and Karoly D J 2015 Are estimates of anthropogenic and natural influences on Australia's extreme 2010–2012 rainfal model-dependent? *Clim. Dyn.* **45** 679–95

Meehl G A *et al* 2013 Climate change projections in CESM1 (CAM5) compared to CCSM4 *J. Clim.* **26** 6287–308

Min S-K, Zhang X, Zwiers F W and Hegerl G C 2011 Human contribution to more-intense precipitation extremes *Nature* **470** 378–81

Min S K, Zhang X, Zwiers F, Shiogama H, Tung Y S and Wehner M 2013 Multimodel detection and attribution of extreme temperature changes *J. Clim.* **26** 7430–51

Morice C P *et al* 2012 Quantifying uncertainties in global and regional temperature change using an ensemble of observational estimates: the HadCRUT4 dataset *J. Geophys. Res.* **117**

NCAR 2012 The NCAR command language [Software]. 6.0.0 edn UCAR/NCAR/CISL/VETS, Boulder, CO

Otto F E L *et al* 2012 Reconciling two approaches to attribution of the 2010 Russian heat wave *Geophys. Res. Lett* **39** L04702

Pall P, Aina T, Stone D A, Stott P A, Nozawa T, Hilberts A G and Allen M R 2011 Anthropogenic greenhouse gas contribution to flood risk in England and wales inautumn 2000 *Nature* **470** 382–5

Perkins S E *et al* 2012 Increasing frequency, intensity and duration of observed global heatwaves and warm spells *Geophys. Res. Lett* **39** L20714

Rahmstorf S and Coumou D 2011 Increase of extreme events in a warming world *Proc. Natl Acad. Sci. USA* **108** 17905–9

Shiogama H, Watanabe M, Imada Y, Mori M, Kamae Y, Ishii M and Kimoto M 2014 Attribution of the June-July 2013 heat wave in the southwestern United States *SOLA* **10** 122–6

Shiogama H, Watanabe M, Imada Y, Mori M, Ishii M and Kimoto M 2013 An event attribution of the 2010 drought in the South amazon region using the MIROC5 model *Atmos. Sci. Lett.* **14** 170–5

Sillmann J, Kharin V, Zwiers F, Zhang X and Bronaugh D 2013 Climate extremes indices in the CMIP5 multimodel ensemble: part 2. Future climate projections *J. Geophys. Res.* **118** 2473–93

Stott P A, Stone D A and Allen M R 2004 Human contribution to the European heatwave of 2003 *Nature* **432** 610–4

Stone D A and Allen M R 2005 The end-to-end attribution problem: from emissions to impacts *Clim. Change* **71** 303–18

Stone D A and Pall P 2016 A benchmark estimate of the effect of anthropogenic emissions on the ocean surface. *J. Adv. Model. Earth. Sys.* submitted

Sun Y *et al* 2014 Rapid increase in the risk of extreme summer heat in Eastern China *Nat. Clim. Change* **4** 1082–5

Taylor K E, Stouffer R J, and Meehl G A 2012 An overview of CMIP5 and the experiment design *Bull. Am. Meterol. Soc.* **93** 485–98

Wen H Q, Zhang X, Xu Y and Wang B 2013 Detecting human influence on extreme temperatures in China *Geophys. Res. Lett.* **40** 1171–6

Wolski P, Stone D, Tadross M, Wehner M and Hewitson B 2014 Attribution of floods in the okavango basin, Southern Africa *J. Hydrol.* **511** 350–8

Zhang X, Wan H, Zwiers F W, Hegerl G C and Min S K 2013 Attributing intensification of precipitation extremes to human influence *Geophys. Res. Lett.* **40** 5252–7

Zhou T, Ma S and Zou L 2014 Understanding a hot summer in central eastern China: summer 2013 in context of multi-model trend analysis *Bull. Am. Meteorol. Soc.* **95** S54–7